Co/Pt(110) interface: An x-ray-diffraction study

E. Lundgren,* J. Alvarez, X. Torrelles,† K. F. Peters, H. Isern,‡ and S. Ferrer
European Synchrotron Radiation Facility, Boîte Postale 220, 38043 Grenoble Cedex, France
(Received 15 July 1998; revised manuscript received 5 October 1998)

Surface x-ray diffraction has been used to investigate the growth and structure of thin cobalt deposits on a Pt(110) substrate. The substrate exhibits the missing-row reconstruction, which has been checked and refined with crystallographic measurements. Co grows in the Stranski-Krastanov mode: an initial two-dimensional growth followed by three-dimensional crystallites. In the early growth stages, cobalt fills the missing-row sites and mixes with Pt. Subsequent growth results in the formation of long triangular prisms with the largest side in contact with the substrate. These crystallites have the fcc structure and their lateral faces are 111 planes. [S0163-1829(99)09603-4]

I. INTRODUCTION

Cobalt/platinum multilayers or thin-film alloys have received a great deal of attention in the last few years as magneto-optical recording media due to their large magneto-optical signals and perpendicular anisotropy.[1] Generally speaking, the magnetic interfacial anisotropy arises from a combination of structural and morphological parameters of the film. A great deal of research is being devoted to relate these parameters to the magnetic properties. The most commonly investigated interface is Co/Pt(111), which exhibits several surface structures and alloy formation at the interface.[2–4] In this paper, we present results on Co/Pt(110) since the inherent crystalline anisotropy of the (110) planes of the fcc substrate makes this system an interesting candidate as model to try to disentangle the role of the different structural effects on the interface magnetism. The growth and interfacial atomic structure have been investigated with x-ray diffraction. In short, it was found that the growth mode is Stranski-Krastanov, that there is some intermixing at the interface and that the crystallites, which appear after deposition of several layers are triangular prisms and have the fcc structure. In a forthcoming paper, the results of surface magnetic x-ray diffraction experiments on this system will be presented. Section II gives the experimental details; in Sec. III, a crystallographic study of the clean substrate and that of three atomic layers of cobalt on the Pt(110) substrate is presented. Section IV describes the results on the structure and morphology of the crystallites.

II. EXPERIMENTAL DETAILS

The experiments have been made at the surface diffraction beamline of the ESRF, as previously described.[5] The end station basically consists of a high-precision diffractometer coupled to a UHV chamber containing facilities for sample preparation and characterization including several evaporators for film growth. The clean crystal surface was prepared by a combination of argon sputtering and annealing cycles in O_2 until no contamination could be observed on the surface by Auger electron spectroscopy. During the initial cleaning stages, carbon could be detected on the surface. Furthermore, at this initial stage of the cleaning procedure, a 1×3 reconstruction could be observed, confirming previous findings[6] and indicating that this reconstruction may be impurity stabilized.[7] We concentrated on the 1×2 reconstruction, which is the characteristic of the clean substrate. After the surface was prepared, the dimensions of the surface terraces were of several tens of nm as deduced from the widths of the diffraction peaks. The (110) planes of fcc metals are anisotropic in nature: close-packed rows of atoms run along the $[\bar{1}10]$ direction whereas in the [001] direction the interatomic distance is $\sqrt{2}$ times the nearest-neighbor distances. The crystal lattice has been described with a basis A_1, A_2, A_3 parallel to the $[1\bar{1}0]$, [001], and [110] directions, respectively with $A_1=A_3=a_0/\sqrt{2}$, and $A_2=a_0$ (bulk lattice constant of Pt). The corresponding reciprocal lattice directions are designed as H, K, L, respectively. Bulk Bragg reflections are found at (H,K,L) values with $L=0,2,4,\ldots$ or $L=1,3,5,\ldots$ depending if H and K have the same or different parity. As is customary in surface x-ray diffraction, the L values denote the perpendicular momentum transfer and are continuously varying along the so-called diffraction rods. Cobalt was deposited from an electron-beam evaporator installed in the diffraction chamber. During deposition the pressure was in the 10^{-10}-mbar range.

III. CRYSTALLOGRAPHIC RESULTS

The clean Pt(110) exhibits the well-known missing row reconstruction which has been investigated in the past with low-energy electron diffraction[8] (LEED) and x rays.[9] One of every two compact atomic rows along $[\bar{1}10]$ is missing, causing the subsurface atoms to pair towards the missing-row position. In order to check and try to refine the structural parameters determined in the past, a crystallographic set of data was collected from the clean surface. That was done by measuring the integrated intensities obtained upon rocking the surface around its normal and by applying the necessary corrections.[10] Four fractional order rods characteristic of the reconstructed surface (H integer, K half integer) and three crystal truncation rods (H and K integers) were measured. The total number of nonequivalent reflections was 198. The average uncertainty as estimated from the 38 symmetry equivalent reflections was found to be 9%. In Fig. 1, two

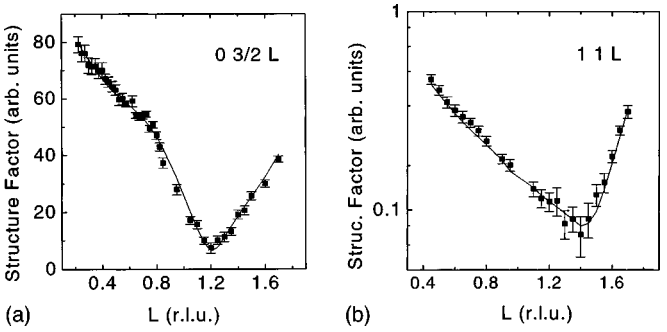

FIG. 1. The structure factor of (HK) reflections as a function of the perpendicular momentum transfer L for the clean (1×2) reconstructed missing-row Pt(110) surface. (a) The $(0\ -3/2\ L)$ fractional order rod. (b) The $(1\ 1\ L)$ crystal truncation rod. The circles are the data points, the continuous curves are the best fits to the data.

rods are shown as representative examples of the measurements: the $(0\ -3/2\ L)$ and the $(1\ 1\ L)$. The solid curves in the figures represent the optimum fit to the data. The optimum atomic positions, as found by using a χ^2 minimization method, starting from the missing-row model, are in good agreement with the earlier work.[8,9] We found that the interplanar distance between the two topmost planes is contracted—0.27 ± 0.1 Å respect to the bulk. The second and third layers have the same separation as found in the crystal bulk. On the second layer, adjacent rows of atoms are displaced by 0.12 ± 0.06 Å towards each other (along A_2) relative to the bulk. The pairing in the third layer amounts to 0.04 ± 0.02 Å. Also, a very small buckling of 0.02 ± 0.02 Å of the atoms directly underneath the missing rows emerges from the fit. The only significant difference between our results and Refs. 8 and 9 is the magnitude of the relaxation of the interplanar spacing between the second and third layers: the previous x-ray work reported -0.11 Å and the LEED measurements -0.01 Å, the latter being in agreement with our finding. Our optimum structure produced a χ^2 value of 1.8.

After preparing a good reconstructed surface, cobalt was deposited on the substrate at room temperature at a constant evaporation rate (~0.8 atomic layers per minute). To investigate the growth mode of the cobalt deposits, the temporal evolution of the diffracted intensity at $(H,K,L)=(0,0,0.6)$ was measured during evaporation. The value of L was chosen as a compromise between surface sensitivity and diffracted intensity. The highest surface sensitivity occurs at $L=1$ but the diffracted intensity, at this value of L, is too small to do practical real-time experiments. If cobalt grew in a perfect layer by layer mode, the intensity should display a nondamped temporal oscillation since the morphology of the surface would be periodic with time. Imperfect growth (a layer starts growing before the previous one has been completed) would cause damped intensity oscillations. The bottom curve in Fig. 2 shows the result of a room-temperature growth: the intensity shows an initial oscillatory behavior that dies out after three oscillations. For comparison it is shown in the top part of the same figure the result of an identical experiment with the sole exception that the substrate orientation was (111). In that case the number of oscillations is double. The Co/Pt(111) system is known to grow

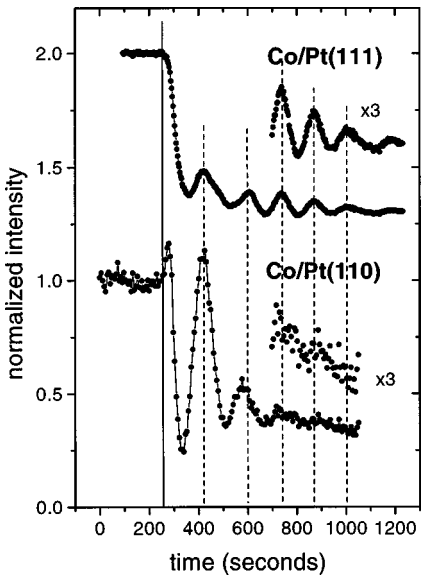

FIG. 2. Temporal evolution of the specularly diffracted intensity during growth of cobalt on Pt(110) (bottom) and on Pt(111) (top) substrates at room temperature. The continuous vertical line indicates the start of the growth. The reduced number of oscillations in the case of Pt(110) evidences three-dimensional growth.

in an imperfect layer by layer mode with several layers growing simultaneously.[2,3] The results displayed in the bottom curve of Fig. 2 are characteristic of a Stranski-Krastanov growth mode: crystallites are formed on the surface after a few layers have grown. The period of the oscillations in Fig. 2 corresponds to the deposition of approximately two atomic layers. This is in contrast with homoepitaxial growth where the period is well known to correspond to the deposition of one atomic layer. The reason for that difference resides in the different atomic numbers of Co and Pt. Simple model calculations of the growth reproduce well the ~2 layer periodicity. An interesting feature of the Co/Pt(110) growth is the initial increase of the diffracted intensity immediately after opening the shutter. The explanation is connected with the missing row reconstruction. The first cobalt atoms arriving onto the surface are likely to adsorb in the positions of the missing Pt atoms causing an increase in the intensity. That picture is confirmed by crystallographic data, as will be shown below.

In an attempt to describe the structure of the Co/Pt interface at the early stages of growth before the Co crystallites dominate the surface structure, we investigated the structure of a film with thickness of approximately three atomic layers (corresponding to the second minimum in the lower curve in Fig. 2), by collecting crystallographic data as was previously done for the clean Pt surface. The situation is more complicated in this case since the growth process causes surface disorder. Also, the intensities of the fractional rods for the Co/Pt surface are weaker than in the clean Pt surface. Five crystal truncation rods and two fractional order rods were measured resulting in 77 independent structure factors. The results are displayed in Fig. 3. By comparing with the data in Fig. 1, one sees that the intensity distributions along the rods are clearly different. To fit the data in Fig. 3, a 1×2 surface cell having two symmetry planes (as in the clean surface) was utilized in order to reduce the complexity of the analy-

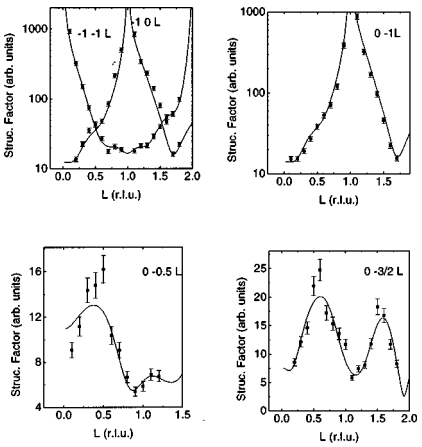

FIG. 3. Structure factor of (1,0) (0,1), (1,1) crystal truncation rods and of (0, 1/2) (0, 3/2) fractional rods for three atomic layers of Co on the Pt substrate. The continuous curves are our best fit to the data.

sis. The surface of the Pt substrate was described with three Pt planes and three Co planes as schematized in Fig. 4. The original missing-row plane is labeled 4 in the figure. The atomic coordinates along the surface normal were described with 12 parameters to investigate possible relaxations. Also, four coordinates along A_2 were allowed to vary. In order to evaluate the possible intermixing of Co and Pt, seven additional parameters were utilized to describe the atomic concentrations at the sites. The total number of parameters in the fit was therefore 25 including scale and roughness. The best fit model ($\chi^2=5$) generates the continuous curves in Fig. 3. Neither the data nor the fit are of the quality that one obtains in a well-ordered and simple surface, preventing an accurate description of the structure of the interface. There are, however, several interesting outcomes. The three topmost layers consist of Co atoms with site occupations of 0.15, 0.48, and 1.0. The partial occupation of the two topmost planes arises from the imperfection in the growth and results in an important surface roughness. The interplanar separations of these Co layers are found to be 6% and 12% smaller than the layer spacing of (110) planes in bulk Pt as indicated in Fig. 4. The relaxations of the A_2 atomic coordinates in the two topmost

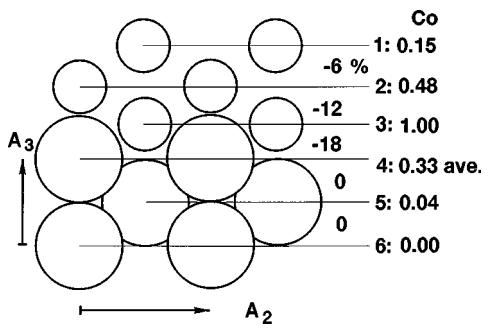

FIG. 4. Schematic representation of the surface cell utilized to model the Co/Pt interface. Small and large circles represent Co and Pt atoms, respectively. Adjacent to the labels of the six atomic planes are the atomic fractions of Co in each layer. Also, the relaxations of the different interplanar distances are indicated. For clarity in the figure, the Co atoms in the interface region have not been drawn.

planes are found to be insignificant. The next atomic plane is the originally missing-row layer. The calculations result in a strong mixing of Co and Pt in that plane: the occupations of the lattice sites are found to be 0.39Co/0.61Pt and 0.26Co/0.74Pt. The interlayer separation between layer three and layer four is contracted at 18%. In fact, layer four is not flat since the Co atoms are found 0.4 Å above the mean z coordinate of the layer (obtained by weighting the individual z coordinates of the atoms with the corresponding site occupations) whereas Pt atoms are 0.2 Å below. The next atomic plane consists almost exclusively of Pt atoms since the occupations of the sites are found to be 0.04 Co/0.96 Pt. The interplanar separation between layers five and four shows no relaxation. Finally, layer number six is identical to a bulk plane. We estimated the error bars in the values of the atomic concentrations and atomic coordinates to be around $\pm 5\%$. Our fit results in large values of the relaxations of the interplanar distances. Specifically, at the interface between Co and Pt we found a contraction of 18%, which resembles previously published results from a LEED study on PtCo(110) alloys.[11] In that case, a contraction of 16% was obtained for the topmost interlayer spacing. As mentioned above, the Co/Pt(110) interface exhibits a 1×2 unit cell as the clean Pt(110) surface. However, the large differences between the rod $(0\ \ 3/2\ \ L)$ in the clean (Fig. 1) and Co covered (Fig. 3) surfaces immediately suggest that the nature of the periodicity doubling is different in both cases. In the Co/Pt system, the non-zero intensity at the fractional order rods arises from the incomplete mixing in the original missing row plane since one atomic row is richer in Pt than the other. The calculations show that the intensity drops practically to zero if both atomic rows have the same stoichiometry. A rather intriguing outcome of our model, is that in the originally missing row plane, the fit gives a Pt atomic concentration of $0.61+0.74=1.35$, which is larger than one, even by taking into account the error bars. A possible explanation for this result is that the missing row reconstruction is not ideal in the starting surface but that some unreconstructed areas would exist, which would contribute to the intensities of the integer order rods causing an excess of Pt in the best fit model. Finally, another question worth mentioning from our fit concerns the Co coverage. As mentioned above, approximately three Co layers were deposited on the surface. The error on the above value may be estimated to be smaller that 0.5 layers. Our best fit model gives a total Co concentration of only two atomic layers as obtained by adding the occupancies of the lattice sites, which is smaller than expected. The reason for this discrepancy has to be found on the existence of a substantial concentration of disordered Co atoms, which are not sitting in lattice sites and that contribute to the diffracted intensity as diffuse background. Similar effects were found in our previous work on Co/Pt(111).[3] In summary, room-temperature deposition of Co on the 1×2 Pt(110) surface, causes the filling of the original missing row sites and a strong mixing with Pt in that plane. In the atomic layers below and above, the mixing is very small. The interface layer develops a significant atomic corrugation and an important interplanar relaxation.

IV. STRUCTURE AND MORPHOLOGY OF THE Co CRYSTALLITES

After depositing approximately six atomic layers of cobalt, diffraction measurements were performed to investigate

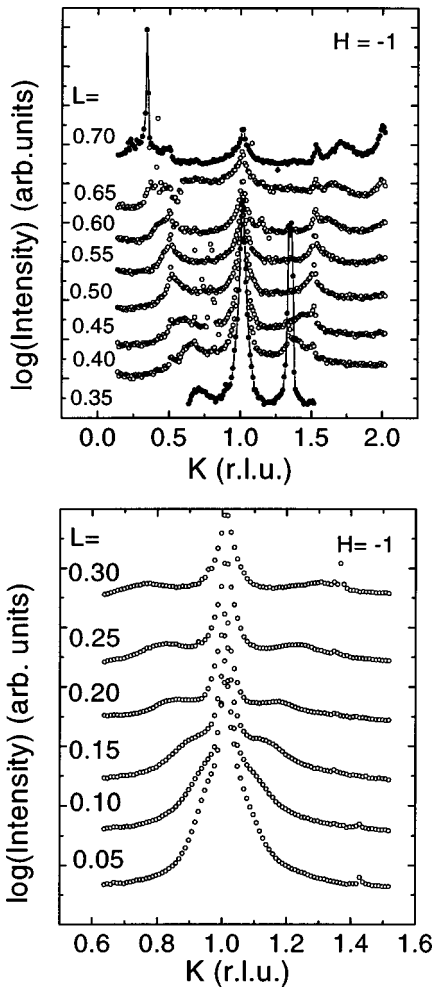

FIG. 5. K scans at different values of L for six atomic layers of Co on Pt(110). The satellites at each side of $K=1$ arise from the triangular facets of the Co crystallites. The intense peaks in the scans with solid data points are bulk-type diffraction reflections from the crystallites.

the morphology of the three-dimensional cobalt clusters. A representative set of data is shown in Fig. 5, which displays a series of scans along K at $H=-1$ and L varying from 0.05 to 0.7. The intensity at $K=1$ decreases upon increasing L since at $(H,K,L)=(-1,1,0)$ there is a bulk Bragg reflection and the minimum intensity in this rod occurs at $L\sim 1$. As it may be seen in the figure, in addition to the peak at $K=1$, two additional peaks appear one at each side. These peaks move apart from each other when L increases. Figure 6 shows the positions of their maxima in the K-L plane as determined by numerical fitting of the scans and the straight lines, which fit the data points. The slopes are -1.03 ± 0.04 and 0.96 ± 0.03. The intersections of the lines in the figure with $L=0$ are found to be 1.07 ± 0.04 and 0.96 ± 0.04. The satellites in Fig. 4 result from diffraction from the Co crystallites. Similar results have been obtained recently in other systems.[12] The lines in Fig. 6 correspond to the directions of the normals to the faces of the crystallites. Within our experimental accuracy both lines have the same slope, which is equal to $\pm 1.00\pm 0.05$. This implies that the angle between the normal of a crystallite face and the A_2 direction is $\tan^{-1}(\sqrt{2})=54.7°$ (the $\sqrt{2}$ results from the ratio A_2/A_3).

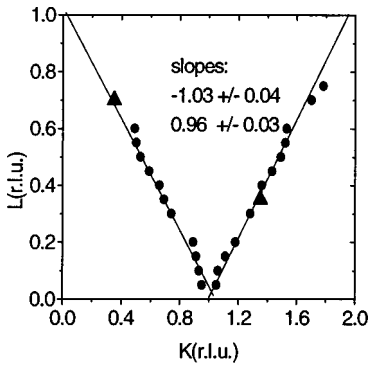

FIG. 6. Position of the maxima of the satellites of Fig. 4 in the K-L plane. The slopes of the straight lines through the data are also indicated. The triangular symbols indicate the intense satellites mentioned in Fig. 5.

The error bar in the slope gives an error bar of $\pm 1.3°$ in the angle. Therefore, the angle of the crystallite faces is twice the above value, which corresponds precisely to the angle defined by the faces (111) and $(1,1,-1)$ (in cubic lattice coordinates) of a fcc crystal. Figure 7 schematizes the geometry of the clusters. The above result is a strong indication of crystallites with the fcc structure. For comparison, if the apex angle of the crystallites were 120° instead of 109.5, as one could guess if the crystallite structure were hcp, one would obtain as L vs K slopes 1.22, which is certainly far from the slopes in Fig. 6. Further insight on the fcc structure can be obtained from our data. Figure 5 shows that the satellites become very intense at $(K,L)=(1.35,0.35)$ and $(0.35,0.70)$ (see the scans with filled data points). The reason for these intense peaks is that they are bulk derived reflections from the stack of the (111) planes of the crystallites. In a perfect stack, *ABCABC*, of fcc planes, the periodicity in the direction normal to the planes is three times the interplanar separation. If in addition to the correct packing, the twin stack *ACB* also occurs, then the crystal has sequences of planes as *ABCACB*, which result in new periodicities in the growth direction. As a consequence, new Bragg reflections are found at $\frac{1}{3}$ or $\frac{2}{3}$ of the reflections corresponding to the perfect stack of planes. It may be easily shown that these new reflections correspond to the intense satellites in Fig. 5. Their existence evidences defects in the stack of Co planes.

In summary, the Co crystallites have the fcc structure and a triangular shape in the A_2,A_3 plane. The side faces are compact (111) cubic type of planes forming an angle of 109.5°.

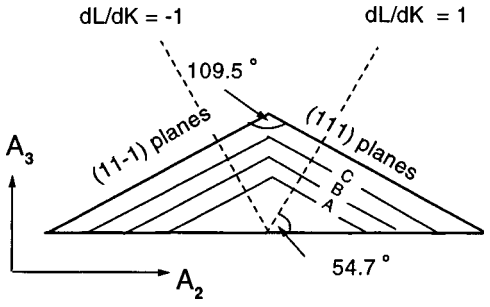

FIG. 7. Geometrical aspect and crystallographic planes in the crystallites.

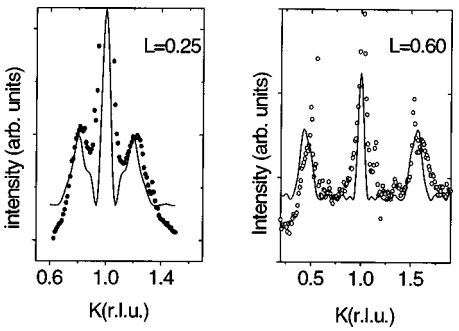

FIG. 8. Data points: closer view of two of the scans in Fig. 4. The continuous lines are calculated from a fcc Co crystallite.

As discussed in Ref. 12, the relative intensities of the satellite peaks coming from the crystallites provide information on the strain distribution inside them. If for a given value of L, the intensities are equal, the strain field, if it exists, is uniform. If they are different then the clusters have a nonuniformly lattice spacing. Visual inspection of the data in Fig. 4 shows that the intensities are very similar (except for the scans with filled data points which have to be considered separately). More detailed information may be extracted by evaluating the diffracted intensity from a model crystallite. The continuous curves in Fig. 8 result from crystallites having 13 atoms at the base and a uniform atomic periodicity along the A_3 direction. As it may be seen the fit is good, since the positions, widths, and intensities of the satellites are well reproduced. The calculation has not included the contribution of the Pt substrate, which produces additional diffracted intensity at $K=0.5$, 1.0, and 1.5.

In order to evaluate the overall dimensions of the crystallites, detailed scans in the H-K planes were performed. It was found that the width of the distribution of diffracted intensity along the K axis was about six times that along the H axis indicating that the crystallites are elongated along A_1. Therefore, the approximate average dimensions of the crystallites in the A_1, A_2, A_3 directions are respectively 216, 47, and 17 Å .

An important question concerning the crystallites remains to be answered. Are the prysmatic crystallites on the surface or are they embedded inside the substrate? A previous scanning tunneling microscopy (STM) study of the growth of Cu on Ni(100),[13] revealed that Cu forms wedges inside the Ni substrate. They were shaped as triangular prisms with internal (111) facets extremelly similar to our findings. It might be possible that the crystallites in the Co/Pt(110) system investigated in the present study are not protruding outside the crystal surface but they are internal wedges as the result of an internal faceting mechanism as in Cu/Ni(100). This question could be answered by STM measurements on Co/Pt(110).

*Permanent address: Institut f. Allgemeine Physik, T.U. Wien, Wien, Austria.
†Also at Inst. Ciencia de Materiales, CSIC, 08193 Bellaterra, Spain.
‡Also at Inst. Ciencia de Materiales, CSIC, Cantoblanco 28049, Spain.

[1] W. J. M de Jonge. P. J. H. Bloemen, and F. J. A. den Broeder, in *Ultrathin Magnetic Structures I*, edited by J. A. C. Bland and B. Heinrich (Springer-Verlag, Berlin, 1994).
[2] P. Grutter and U. T. Durig, Phys. Rev. B **49**, 2021 (1994).
[3] S. Ferrer, J. Alvarez, E. Lundgren, X. Torrelles, P. Fajardo, and F. Boscherini, Phys. Rev. B **56**, 9848 (1997).
[4] J. S. Tsay and C. S. Shern, Surf. Sci. **396**, 313 (1998).
[5] S. Ferrer and F. Comin, Rev. Sci. Instrum. **66**, 1674 (1995).
[6] P. Fery, W. Moritz, and D. Wolf, Phys. Rev. B **38**, 7275 (1988).
[7] M. Mundschau and R. Vanselow, Phys. Rev. Lett. **53**, 1084 (1984).
[8] E. C. Sowa, M. A. van Hove, and D. L. Adams, Surf. Sci. **199**, 174 (1988).
[9] E. Vlieg, I. K. Robinson, and K. Kern, Surf. Sci. **233**, 248 (1990).
[10] For a review see I. K. Robinson, in *Handbook of Synchrotron Radiation Vol. 3*, edited by G. Brown and D. E. Moncton (Elsevier Science Publishers, Amsterdam, 1991).
[11] J. M. Bugnard, Y. Gauthier, and R. Baudoing-Savois, Surf. Sci. **344**, 42 (1995).
[12] A. J. Steinfort, P. M. L. O. Scholte, A. Ettema, F. Tuinstra, M. Nielsen, E. Landemark, D. M. Smilgies, R. Feidenhansl, G. Fakenberg, L. Seehofer, and R. L. Johnson, Phys. Rev. Lett. **77**, 2009 (1996).
[13] B. Muller, B. Fischer, L. Nedelmann, A. Fricke, and K. Kern, Phys. Rev. Lett. **76**, 2358 (1996).